JOURNAL OF CATALYSIS 105, 319–334 (1987)

Manganese-Oxide-Supported Iron Fischer–Tropsch Synthesis Catalysts: Physical and Catalytic Characterization

K. M. KREITMAN,[1] M. BAERNS,[2] AND J. B. BUTT[3]

Ipatieff Laboratory and Department of Chemical Engineering, Northwestern University, Evanston, Illinois 60201

Received June 3, 1986; revised January 14, 1987

It has been claimed that catalysts containing iron and manganese are especially selective for production of low molecular weight olefins in the Fischer–Tropsch (FT) synthesis. In this study a new system, manganese-oxide-supported iron, Fe/MnO, was prepared, subjected to various calcination and reduction treatments, and then employed as a FT catalyst. Reaction studies were run with approximately 1/1 : CO/H_2 feed at 515 and 540 K and 7.8 and 14.8 bar pressure. Although low conversions were employed, the synthesis rate decreased strongly with increasing conversion. Compared to conventional Fe catalysts, the Fe/MnO was more active for water–gas shift and less selective for methane and alcohols, especially at higher conversions, lower temperature, and higher pressure. Olefin selectivity was high, hydrogen chemisorption was depressed, and secondary hydrogenation was not apparent. In general it is concluded that the manganese-supported iron does promote FT selectivity for low molecular weight olefins, but at the expense of high CO_2 formation.

INTRODUCTION

It has been claimed, not without dispute, that Fischer–Tropsch (FT) catalysts based on the FeMn system yield high selectivity to low molecular weight olefins. Though coprecipitated FeMn catalysts have been studied rather extensively, little work has been reported on supported materials, especially at pressures above one atmosphere. The system investigated here was iron on low area manganese (II) oxide. This material is of interest since its FT behavior is highly sensitive to variations in pretreatment conditions, suggestive of a strong metal–support interaction (SMSI).

Product distributions in FT synthesis are normally represented in terms of the Schulz–Flory–Anderson distribution, which gives a linear relationship between the carbon number (n) and the logarithm of the product mole fraction. A common interpretation is growth via surface intermediates of C_i at each step in the chain; a discussion of the limitations imposed by this model is given by Madon (*1*). Breaks in this distribution for high molecular weight products have been demonstrated and attributed to the existence of two types of catalytic sites with different growth probabilities (*1, 3, 4*).

Deviations from the normal product distribution relationship have been observed for FeMn catalysts. Koelbel and Tillmetz (*5, 6*) worked with coprecipitated iron–manganese catalysts with Mn/Fe ratios up to 9 in fixed bed applications. At pressures up to 10.6 bar methane was strongly depressed for high Mn catalysts and the olefin content of the products ranged from 60 to 90%. These results have been supported by the studies of Buessmeier *et al.* (*7, 8*), with particular selectivity for low molecular weight olefins obtained with CO-rich feeds (CO/H_2 = 1 to 1.7). Other recent studies reporting in-

[1] Present address: Shell Development Company, Houston, TX 77001.

[2] Lehrstuhl für Technische Chemie, Ruhr-Universität Bochum, 4630 Bochum—1, West Germany.

[3] To whom correspondence should be addressed.

0021-9517/87 $3.00

creased olefin selectivity have been given by Barrault *et al.* (*9*), Maiti *et al.* (*10*), and Jensen and Massoth (*11*). On the other hand, van Dijk *et al.* (*12*), Deckwer *et al.* (*13, 14*), and Satterfield and Stenger (*15*) report no great enhancement in olefin selectivity with FeMn. In at least the last two cases, however, well mixed reactors at high conversions were employed, so the possibility of olefin hydrogenation was high.

In balance there appears to be substantial evidence for the promotion of olefin selectivity by the incorporation of Mn in iron-based FT catalysts, possibly by the suppression of secondary hydrogenation. In addition, there seems to be some depression of methane formation which is of interest itself with respect to the possibility of an independent pathway for C_1 formation (*16*).

EXPERIMENTAL

Catalysts and reaction. The Fe/MnO catalysts used in this study were prepared by impregnation of a low surface area manganous oxide powder with aqueous ferric nitrate. The MnO, from Alfa Chemicals, was of 99.5% purity with the major impurities Mn (IV) and traces of Fe (150 ppm), sulfate (60 ppm), and alkali (80 ppm). Iron nitrate ($Fe(NO_3)_3 \cdot 9H_2O$) was used as received from Mallinckrodt, purity 98.6% with the major impurity Fe(II). Experiments carried out with ^{57}Fe enriched iron were conducted using material from New England Nuclear containing 90% ^{57}Fe and the remainder ^{56}Fe.

The MnO support was further purified by repeated washing in deionized water and 0.2 *N* HNO_3, drying in air at 400 K overnight, calcination at 873 K for 50 h, reduction in H_2 at 793 K, passivation in air at room temperature, then repetition of the washing–drying procedure. After these treatments the BET area was ca. 10 m^2/g and the grain size 80–100 mesh. Impregnation with the ferric nitrate solution was carried out by the incipient wetness method with loadings to correspond to about half of a monolayer. Some small variants from this procedure were required for the ^{57}Fe-containing catalysts, but the total iron content remained the same. After attaining incipient wetness, the material was calcined in air at 473 K for 50 h; the result of this procedure is termed subsequently the "low temperature calcined" (LTC) catalyst. A portion of this material was subsequently air calcined at 773 K for 10 h, i.e., "high temperature calcined" (HTC) catalyst. Iron weight loading and density of the two materials are given in Table 1. The differences between them are due to extensive support oxidation in the HTC material.

Reagent gases used in reduction and in the reaction studies were similar to those used previously (*17*). The reactant gas was a mixture of CO/H_2: 1.16/1 supplied by Airco in aluminum cylinders to minimize carbonyl impurity. Possible carbonyl impurities were further removed on-line by decomposition in a large volume silica bed heated to 430 K. The design of the differential flow reactor used in reaction experiments was similar to that of Acuri *et al.* (*17*) with some modifications as described in (*18*). One experiment was run with 99% pure propene incorporated in the standard $CO:H_2$ mixture to the extent of 2.5% to check possible olefin hydrogenation and/or incorporation in chain growth.

Two types of catalyst reduction procedures were employed, both using H_2 at 1 bar. The "standard reduction" method was to increase temperature to 793 K over a period of 5 h in an H_2 flow of about 2000 vol gas (RTP)/vol reduced catalyst-h (v/v-h). In the second method ("fast reduction") the temperature was raised to 793 K in about 60 min at an H_2 flow of 800. In both methods

TABLE 1

Fe/MnO Catalysts

Catalyst	Calcination, K	Iron, wt%	Density, g/cm³
LTC	473	2.14	2.0
HTC	773	1.95	2.2

after the initial treatment H_2 was maintained for 24 h, after which the reactor was cooled to 473 K and the reaction procedure initiated. Reaction experiments normally lasted for 80–90 h, with temperatures maintained to within ±0.5 K and at total pressures of 7.9 or 14.8 bar. The rather long times required for equilibration of higher molecular weight products was allowed for by providing a 24-h run-in period before any reaction data were considered to be at steady state. There was a moderate loss of activity associated with the equilibration, but activity maintenance thereafter was very good and deactivation is not a factor in the results reported here. Product analysis procedures were similar to those of (*17*), with a few differences in detail given in (*18*).

Mössbauer characterization. Specific Mössbauer studies of the FeMn system have been reported by Jaggi *et al.* (*19*) and Deppe *et al.* (*20*). The apparatus used in this work is as described before (*19*), with samples enriched in ^{57}Fe. Spectra were accumulated *in situ* after pretreatment, without initial passivation of the catalyst in air, and were recorded in the transmission mode with the source and absorber at room temperature.

X-ray diffraction characterization. Diffraction experiments were performed on an automated Rigaku diffractometer. Chromium K_α radiation was used to avoid excessive fluorescence by the manganese and, in view of the high ratio of MnO to Fe in the samples, a vanadium filter was employed to remove selectively the K_β line.

RESULTS: CATALYTIC CHARACTERIZATION OF Fe/MnO

The bulk of results given here refer to experiments at 515 K and low CO conversions (<10%) under conditions of no diffusional limitations. Conversion level was varied by changes in reactor space velocity, and experiments at differing conversions were not conducted in fixed order. The effect of catalyst pretreatment, LTC and HTC, was included in the investigation.

The terms "CO conversion, FT rate, and selectivity" refer to primary Fischer–Tropsch reactions, that is the production of hydrocarbons and alcohols. Results are presented on the basis of C_1–C_7 hydrocarbon and C_1–C_2 alcohol analysis after the initial stabilization period. Selectivity is defined further as the ratio of CO converted to product *i* to total CO converted to primary FT products.

Effect of CO conversion level. All of the Fe/MnO catalysts investigated are qualitatively similar, with rate decreasing with increasing conversion. This is similar to Fe/SiO_2, but differs from the results reported by Dry *et al.* (*21*). Typical data are illustrated in Fig. 1.

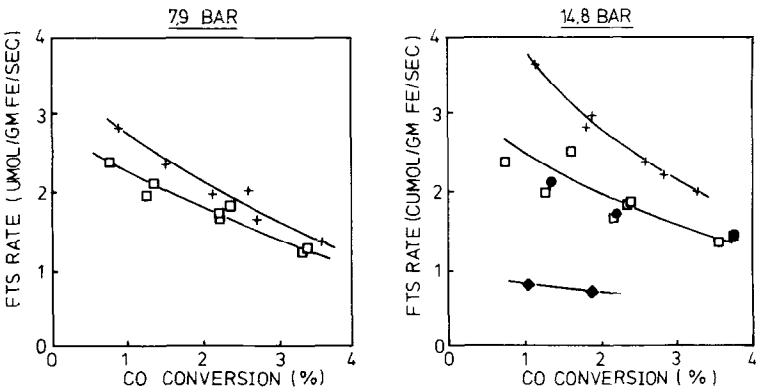

FIG. 1. Synthesis activity (CO to primary products) as a function of CO conversion at 515 K. (+) LTC; (□) HTC; (●) HTC, propene enhanced; (◆) HTC, fast reduction.

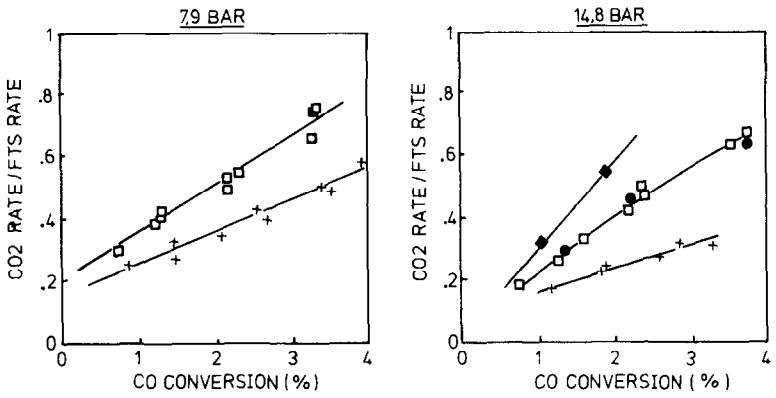

FIG. 2. Relative CO_2 production as a function of CO conversion at 515 K. Symbols are as in Fig. 1.

CO_2 is generally considered to be a secondary product (*21, 22*), which accords with the results for Fe/MnO shown in Fig. 2. While the ratio of CO_2 production to FT synthesis rate increases with increasing conversion, the ratios are high compared to similar Fe/SiO_2 catalysts under comparable conditions. We have ruled out disproportionation as the source of CO_2 (*18*) on the basis of separate studies. Thus, high CO_2 is the result of water–gas shift activity and, in fact, shift equilibrium to CO_2 is very favorable under the conditions employed (*23*).

Hydrocarbon selectivity demonstrates different patterns with increasing conversion level. Methane is decreased, C_2–C_4 remains relatively constant, and C_4–C_5 increases. The alcohol selectivities strongly decrease, but in any event are less than $\frac{1}{20}$ total product at a nominal 4% CO conversion. This is much less than comparable unpromoted Fe catalysts (*17*). Methane selectivities are also lower; quantitative results are given in Fig. 3.

The olefin/paraffin distributions are relatively constant with conversion on the Fe/MnO catalysts. Moreover, hydrocarbons up to C_7 are at least 80% olefinic. An example of the magnitude and trends in selectivity is provided in Fig. 4 for C_3.

Effect of reaction pressure. Since pressure variations did not affect all the catalysts in the same way, general observations are limited to the following:

(1) The relative CO_2 production rate decreases with increasing pressure. As seen in Fig. 2 the slopes of the lines do not change much, but the linearly extrapolated

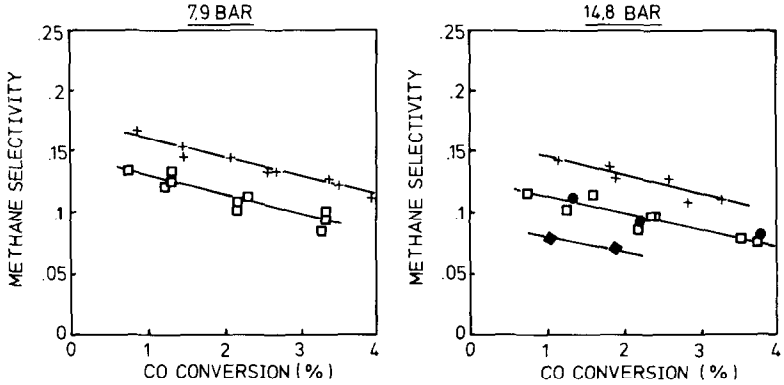

FIG. 3. Selectivity to methane as a function of CO conversion at 515 K. Symbols are as in Fig. 1.

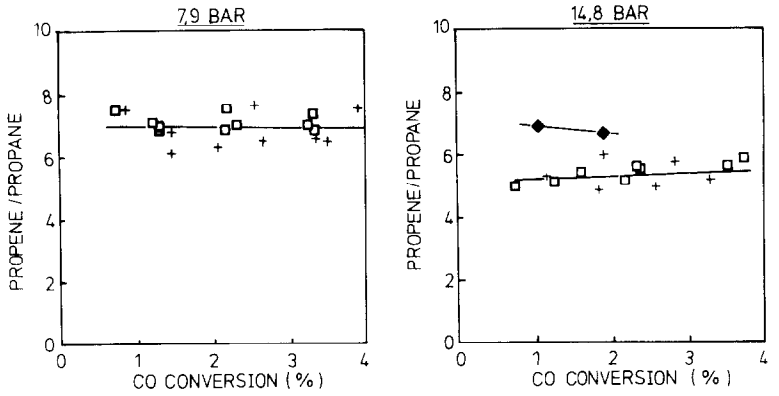

FIG. 4. Propene/propane production ratio as a function of CO conversion at 515 K. Symbols are as in Fig. 1.

zero conversion intercept is higher at lower pressure. Possibly there is some primary oxygen removal that disappears at higher pressure.

(2) Increasing pressure causes the methane selectivity (Fig. 3) and the olefin/paraffin ratio (Fig. 4) to decrease. Higher hydrocarbons also become less olefinic.

(3) Increasing pressure tends to enhance the differences in behavior between LTC and HTC catalysts.

Reaction rates. Attempts were made to measure the chemisorption of hydrogen on the Fe/MnO catalysts using the method of Amelse *et al.* (*24*). Unfortunately, quantitatively reliable results could not be obtained. Spillover onto the MnO is very high and chemisorption is obviously severely repressed relative to comparable Fe/SiO_2, indicative of a strong metal–support interaction, as discussed later. Given this situation for the low surface area materials studied here we can only say that hydrogen chemisorption was very low and the rates of reaction are thus based on total Fe loading.

Calcination temperature. In Fig. 1 it is seen that the synthesis rates are lower over HTC than LTC catalysts. The HTC catalysts also give higher CO_2 yields, as seen in Fig. 2. Other differences between HTC and LTC catalysts are:

(1) lower C_1 selectivity (Fig. 3),
(2) higher C_4 selectivity,
(3) lower methanol selectivity (Fig. 5),
(4) higher ethane/ethane ratio.

At 7.9 bar all other selectivities, as shown in these figures, are comparable. However, at the higher pressure of 14.8 bar the fol-

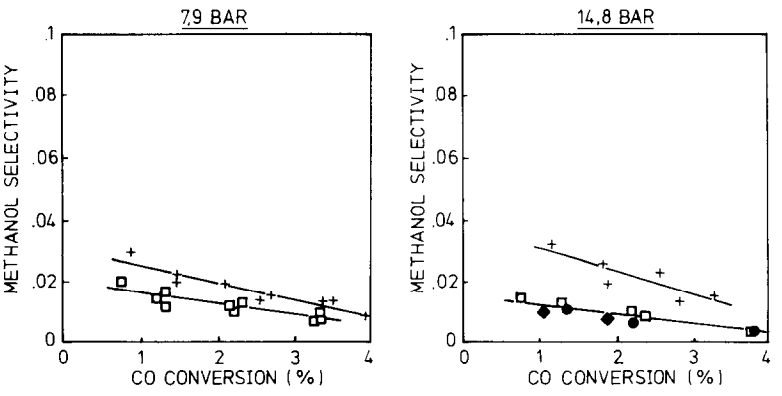

FIG. 5. Selectivity to methanol as a function of CO conversion at 515 K. Symbols are as in Fig. 1.

lowing can be added to the list of differences:

(1) There is about a 10–15% increase in C_2-C_5 selectivity.

(2) HTC decreases alcohol selectivity, as shown in Fig. 5 for methanol. Similar trends are observed for ethanol with about the same percentage reduction (*18*).

Thus, pressure variation affects the two Fe/MnO catalysts differently. For the HTC catalyst increasing pressure has little effect on the overall FT rate, but gives an increase in the C_2-C_4 products and a decrease in alcohols and methane. For the LTC catalyst, increasing pressure results in higher FT rates and an increase in alcohols at the expense of methane.

Reduction procedure. The results reported to this point refer to catalysts (either LTC or HTC) reduced via the "standard reduction." LTC catalyst behavior was similar when either the standard or fast reduction procedure was used, but HTC catalyst activity was very low and the selectivity altered after use of the fast reduction method. X-ray diffraction results indicate that the LTC catalysts have only a very small amount of MnO oxidation, but HTC catalysts are almost completely converted to the sesquioxide. Therefore, a large amount of water is released during the fast reduction in a short time that could significantly alter the state of the support compared to slow reduction. The following observations can be made about the catalytic behavior at 515 K and 14.8 bar of HTC catalysts reduced by the fast method compared to the standard:

(1) The FT rate is much lower (Fig. 1).

(2) The relative CO_2 rate is higher (Fig. 2).

(3) The methane selectivity is lower (Fig. 3).

(4) Olefin/paraffin ratios are higher (Fig. 4).

In general, the fast reduction procedure amplifies the differences between the HTC and LTC catalysts.

Effect of propene enhanced feed. During these experiments it was noted that a relatively large amount of branched products was formed. For example, isobutene accounted for almost 17% of the C_4 products from the standard reduced HTC catalyst at 14.8 bar. Under similar conditions Fe/SiO_2 produces negligible amounts of isobutene (*17, 25*). Olefin homologation has been proposed as a possible mechanism to explain such branching (*26*). To test this more directly an experiment was performed in which a relatively high concentration of propene (0.36 bar) was added to the feed for a 26-h period, after which normal feed was restored. The results of this experiment are also shown in Figs. 1–5. No measurable modification of activity or selectivity is apparent, although due to the very large amount of propene introduced (~10 times that normally produced) the effect on C_3 production could not be determined. However, the absence of any other effects would seem to rule out any significant amount of homologation, as well as to indicate that the hydrocarbon products are not involved in the inhibition of the FT rate other than via possible competitive adsorption effects. A small amount of olefin incorporation in chain growth has been reported on iron for Fe/SiO_2 catalysts (*27, 28*) but even this is not noted here. Finally, very little (if any) of the propene was hydrogenated. Others have noted extensive hydrogenation in olefin/enhanced feed experiments with typical FT catalysts (*17, 28, 29, 30*); in contrast, with Fe/MnO secondary olefin hydrogenation does not seem important and the small amounts of paraffins formed may be primary products.

Effect of reaction temperature. A series of experiments was run at 540 K in addition to those at 515 K. Most parameters vary in a similar manner with pressure at the two temperatures, with the exception that there is no effect of pressure on a hydrocarbon selectivity or ethene/ethane ratio at 540 K.

The overall synthesis rate increases by almost an order of magnitude, and is even more sensitive to the conversion level, as

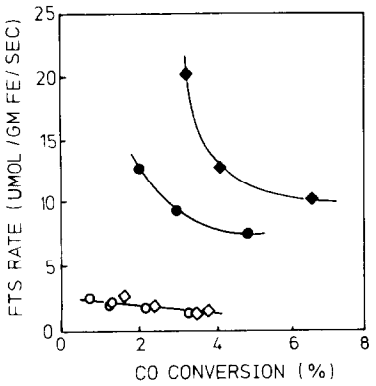

FIG. 6. Synthesis activity as a function of conversion, HTC catalyst, 515, and 540 K. (●) 540 K, 7.9 bar; (◆) 540 K, 14.8 bar; (○) 515 K, 7.9 bar; (◇) 515 K, 14.8 bar.

shown in Fig. 6. The larger rate inhibition at 540 K is puzzling. Even if one assumes inhibition by products to be the same at 515 and 540 K (ca. 4% conversion) the apparent activation energy would still be unreasonably high, about 45–50 kcal/mole. Indeed, the fact is that rate depression by product inhibition probably diminishes at higher temperatures and the conversion dependence of rate originates from other factors. Additional observations as one goes from 515 to 540 K are:

(1) Methane selectivity increases by about 70%.

(2) CO_2 production is about the same.

(3) Alcohol selectivities increase on the order of 20%, but this is not significant given the low selectivities at 515 K. Low alcohol selectivities seem generally characteristic of FeMn systems (*31*).

(4) There are small changes in olefin/paraffin ratios, but again not very significant in view of the overall large change in synthesis rate.

DISCUSSION: CATALYTIC CHARACTERIZATION

There are several important differences between Fe/MnO and unpromoted Fe catalysts. First is the high water–gas shift activity, about five times that of Fe/SiO_2 under similar conditions (*17*). As noted above, equilibrium would be expected at higher conversions. A second important difference is in methane selectivity. At 3% CO conversion, 14.8 bar, and 523 K, a comparable Fe/SiO_2 produced 19% CH_4 on a carbon efficiency basis (*24*), compared to 8% at 515 and only 16% at 540 K on the standard reduced HTC Fe/MnO. Product distributions for Fe catalysts invariably show methane on or above the standard chain growth plots; the opposite for Fe/MnO is shown in Fig. 7 (note that CO_2 is not included in the C_1 count of the figure) for a particular set of results, but it seems general for Fe/MnO. Unfortunately, this is counterbalanced somewhat by high CO_2 formation.

Finally, olefin hydrogenation is much less evident for Fe/MnO than for unpromoted catalysts. Though both are good olefin producers at low conversions, it would be expected that Fe/MnO retains olefin selectivity better at higher conversions (*31*).

If these three criteria (high shift activity, lowered methane selectivity, and high olefin/paraffin ratio) can be taken as a measure of promotion shown by Fe/MnO, then the general ranking from most to least promotion is:

(1) fast reduced HTC,
(2) standard reduced HTC,
(3) standard reduced LTC.

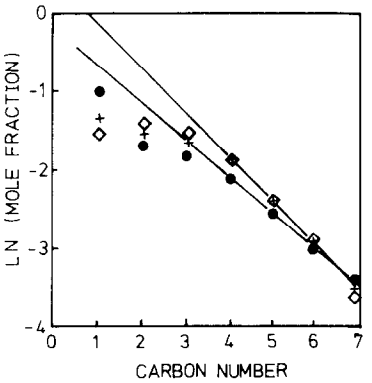

FIG. 7. Effect of pretreatment and CO conversion level on hydrocarbon product distribution at 515 K, 14.8 bar. (+) LTC, 3.8% conversion; (●) LTC, 1.9% conversion; (◇) HTC, fast reduction, 1.9% conversion.

This ranking also corresponds to the lowest to highest overall FT activity. It will be seen that this may well correspond to the concentration of MnO on the iron surface, since if surface MnO stabilizes a more oxidized iron surface there should result higher shift activity and perhaps lower synthesis activity.

The results on methane selectivity invite consideration in terms of two-site models that propose methane formation on FT growth sites as well as on methane-selective sites (*16, 32*). If such methane-selective sites were more susceptible to rate inhibition by products than growth sites, then some aspects of the observed methane selectivity could be understood. However, the situation seems complex for Fe/MnO. Referring again to Fig. 7, as the CO conversion increases methane decreases, but the growth probability for C_4-C_7 products also decreases. Thus in view of the two-site model the rate inhibiting products must, in addition to depressing the activity of the methane-selective sites, either increase the propagation rate or decrease the termination rate of the growth sites. These questions cannot be resolved on the basis of the selectivity data here, so the two-site model is really not of much assistance in interpretation. Such changes in methane selectivity are most certainly affected by pretreatment conditions and are discussed in more detail for conventional FeMn catalysts in Refs. (*18, 31*).

Increasing the pressure on the HTC catalysts at 515 K results in an increase in the ethene/ethane ratio and a large increase in C_2–C_4 selectivity. This may well be due to increased surface–product interactions on the HTC material, but the changes are absent at 540 K. Alcohol selectivities both increase marginally with pressure at 540 K; the behavior seems opposite to those of typical iron catalysts but, as stated before, the alcohol selectivities are so low that it is difficult to ascribe much importance to them.

The addition of a rather large amount of propene to the feed had no measurable effect on the activity and selectivity of the HTC catalyst at 515 K and 14.5 bar. While generalization from a single experiment is usually not wise, this result does tend to indicate that under at least some conditions the products that dictate rate inhibition and selectivity changes are CO_2 and/or H_2O, not hydrocarbons. These may either selectively block or change the oxidation states of the active sites. The overall behavior of Fe/MnO differs from Fe/SiO_2 in that there is no incorporation of olefin in the next highest carbon number product, and no evidence for hydrogenation.

Overall, the results indicate MnO promotion of iron catalysts toward low molecular weight olefins, primarily via a decrease in methane selectivity. However, this is accompanied by a large increase in CO_2 formation. At higher conversions the water–gas shift reaction would be expected to approach equilibrium, thus we have an olefin-selective catalyst that unfortunately also likes the water–gas shift reaction.

RESULTS: PHYSICAL CHARACTERIZATION

The formation of the MnO-supported iron catalysts of this study is a complex process. Unlike typical support materials such as Al_2O_3, MnO is moderately soluble in acid solution. Since iron nitrate is highly acidic, the preparation process is really a localized coimpregnation with iron and manganese nitrates, so support interaction is present from the very beginning of the catalyst preparation. To obtain a better understanding of this, phase distributions of the Fe/MnO were studied in various states using Mössbauer spectroscopy and X-ray diffraction. It is a rather complex problem, as the prior studies of FeMn by Jaggi *et al.* (*19*) and Deppe *et al.* (*20*) have shown. While the calcined materials are of interest, the reduced and carburized species are probably more so, and the discussion centers on the latter two; other details are given in (*18*).

Mössbauer spectroscopy. Transmission

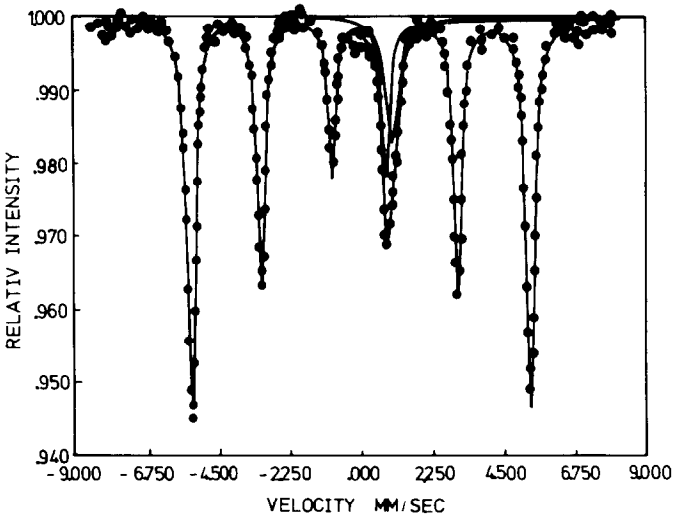

FIG. 8. Mössbauer spectrum of the reduced LTC catalyst.

mode spectra were employed to characterize the iron-containing phases in the catalysts. Materials employed were similar to those used in catalytic characterization, but the ^{57}Fe isotopic fraction was increased by a factor of 6. Catalytic behavior of enriched and nonenriched catalysts was the same. Complete details are given in (*18*). We deal here with the reduced and carbided catalysts.

Spectra of reduced ^{57}Fe-enriched catalysts are shown in Figs. 8 and 9. Both LT and HT samples can be fit as a broad single peak and a sextet, and corresponding Mössbauer parameters are given in Table 2. The single peak at IS ~ 1 mm/sec is most likely an unresolved doublet due to FE(II) in an FeO–MnO solid solution. The sextet is undoubtedly metallic iron, nearly manganese free, due to the tendency for Mn to

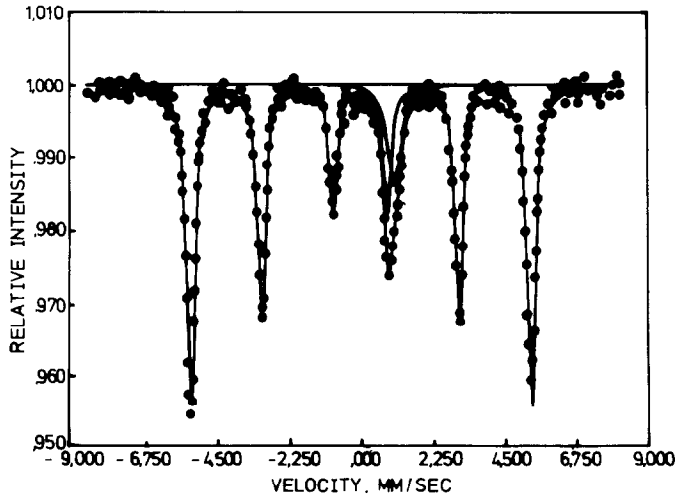

FIG. 9. Mössbauer spectrum of the reduced HTC catalyst.

TABLE 2

Mössbauer Parameters for Reduced Fe/MnO Catalysts[a]

Catalyst sample	Isomer shift (mm/sec)	Quadrupole splitting (mm/sec)	Hyperfine field (κ0)	Area fraction	Phase identification
LTC[b]	0.00	0.02	331.3	0.89	Fe
	1.07	[c]	—	0.11	(Fe,Mn)O
HTC[d]	0.00	0.05	331.6	0.89	Fe
	1.04	[c]	—	0.11	(Fe,Mn)O

[a] ^{57}Fe-enriched catalysts.
[b] Fig. 8.
[c] Unresolved doublet.
[d] Fig. 9.

remain in the divalent state. The extent of reduction of iron for both LTC and HTC catalysts was measured as ~0.85 fraction metallic iron; however, the HTC catalyst under fast reduction conditions was only about 0.60 Fe.

For the carbided catalysts very complex spectra are obtained, many aspects of which have been described in (*19*) and (*20*). Mössbauer spectra of ^{57}Fe-enriched Fe/MnO catalysts after use for the synthesis reaction (515 K) are shown in Figs. 10 and 11. Corresponding Mössbauer parameters are given in Table 3. The HTC catalyst was reduced by the standard method and run under reaction conditions at 7.9 bar for 24 h and then at 14.8 bar for 48 h. The LTC catalyst was treated similarly, but only for 24 h at 14.8 bar. The spectra were fit as combinations of ε'-$Fe_{2.2}C$ and χ-Fe_5C_2 carbides, Fe(II) in (Fe,Mn)O, and iron metal. The calculated carbide distributions in Table 3 have relatively large degrees of uncertainty associated with them, although the area ratios of the three χ-carbide sites are equal to the expected 2 : 2 : 1 (*34*) within experimental error. The hyperfine yield decreases strongly with manganese content (*35*), so it

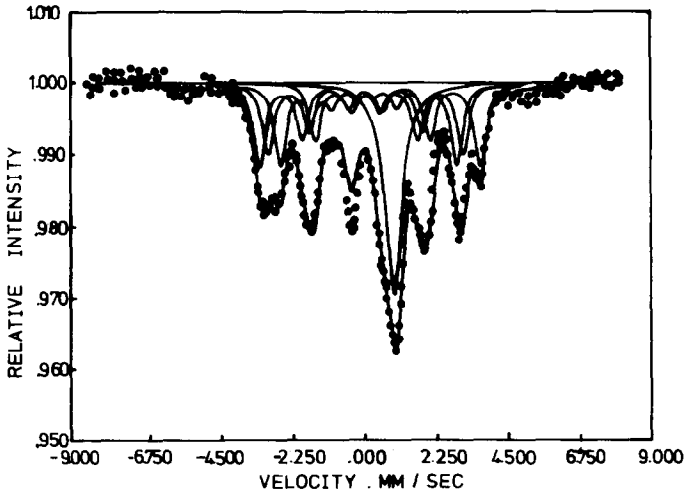

FIG. 10. Mössbauer spectrum of the carbided LTC catalyst.

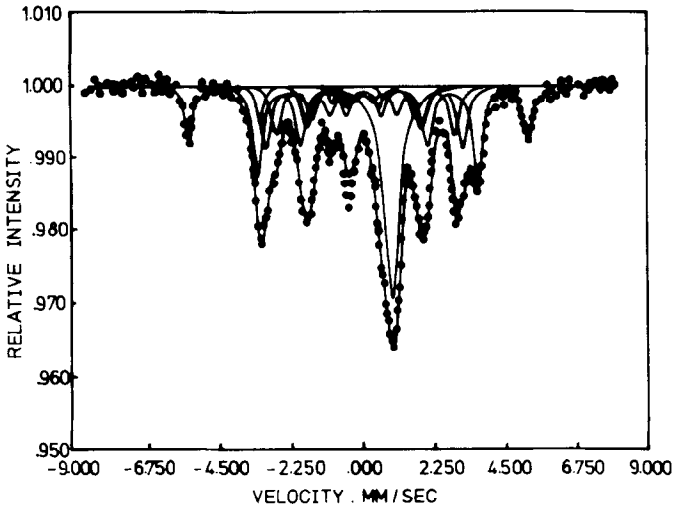

FIG. 11. Mössbauer spectrum of the carbided HTC catalyst.

is concluded that these phases are nearly manganese free. The presence of ε' and χ carbide phases has also been reported by Kim *et al.* (*36*) for Mn-promoted Raney iron synthesis catalysts (T = 453 K, P = 1465 kPa, H_2/CO : 2/1).

An unexpected result is the retention of some uncarbided iron on the HTC catalyst. Similar Fe/SiO_2 catalysts are completely transformed to carbide even at lower CO partial pressures (*37, 38*). There is no strong evidence for the formation of spinel phases (*19, 20, 39*) so a first explanation for this effect is that some of the iron particles of the HTC catalyst are blocked from contact with CO by an overlayer of MnO or of FeO stabilized by the presence of surface MnO.

X-ray diffraction. Wide angle X-ray diffraction was employed to determine the state of the manganese oxide at various stages of treatment and also to obtain some complementary information on iron-containing phases. A detailed identification of

TABLE 3

Mössbauer Parameters for Carbided Fe/MnO Catalysts

Catalyst sample	Isomer shift	Quadrupole splitting	Hyperfine field	Area fraction	Phase identification
LTC	0	0	330.9	0.12	Fe
	0.20	−0.08	173.8	0.14	ε'-$Fe_{2.2}C$
	0.18	−0.07	192.3	0.17	
	0.23	−0.21	213.9	0.24	χ-Fe_5C_2
	0.19	−0.11	112.2	0.11	
	1.03		—	0.22	(Fe, Mn)O
HTC	0.22	−0.13	171.3	0.24	ε'-$Fe_{2.2}C$
	0.16	−0.01	189.2	0.20	
	0.23	−0.23	214.3	0.24	χ-Fe_5C_2
	0.20	−0.24	109.1	0.10	
	1.01		—	0.22	(Fe, Mn)O

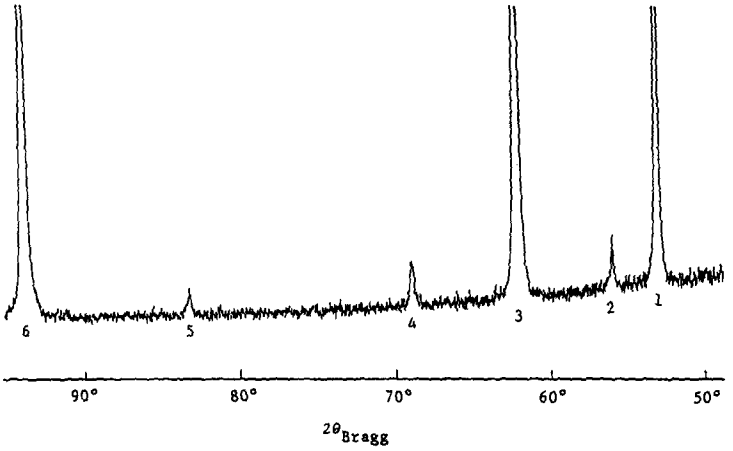

FIG. 12. X-ray diffraction pattern of the reduced LTC catalyst.

	D-spacing (nm)	Peak
(1)	0.257	MnO (111)
(2)	0.222*	MnO (200)
(3)	0.222	MnO (200)
(4)	0.203	Fe (110)
(5)	0.157*	MnO (220)
(6)	0.157	MnO (220)

* Due to incompletely filtered Cr K_β radiation.

phases is given for all catalysts in (*18*); results for the reduced and carburized materials are given here.

Typical diffraction patterns for the reduced LTC catalyst and fast reduced HTC catalyst are given in Figs. 12 and 13. Diffraction patterns for all reduced Fe/MnO catalysts are similar, regardless of calcination or reduction treatment; the major phase is MnO. Any (Fe,Mn)O reflections present are completely obscured by the intense peaks of MnO. An average iron–

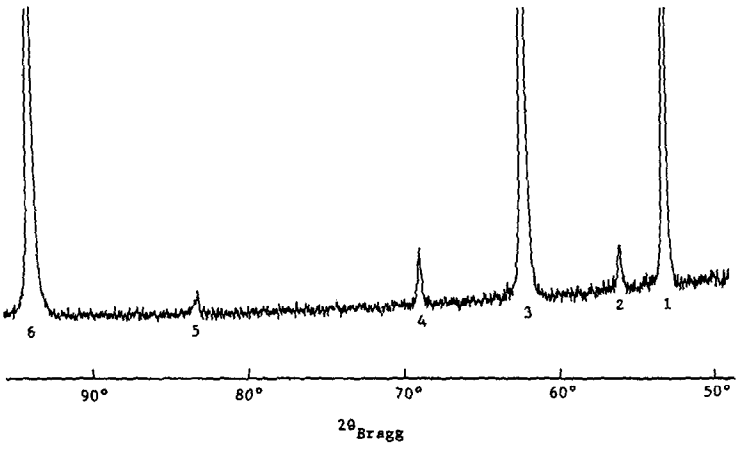

FIG. 13. X-ray diffraction pattern of the fast reduced HTC catalyst (description of peaks as for Fig. 12).

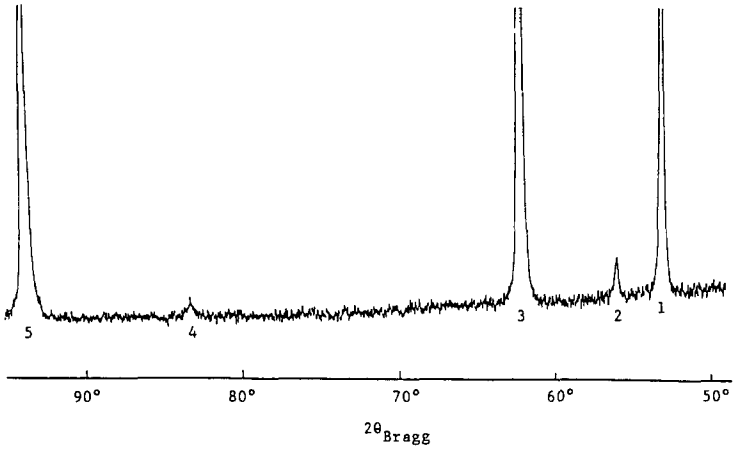

FIG. 14. X-ray diffraction pattern of the carbided HTC catalyst.

	D-spacing (nm)	Peak
(1)	0.257	MnO (111)
(2)	0.222	MnO (200)
(3)	0.222	MnO (200)
(4)	0.157	MnO (220)
(5)	0.157	MnO (220)

metal particle size of 70 nm is estimated using the Scherrer equation.

A representative diffraction pattern from a carbided catalyst is shown in Fig. 14. Due to the distribution of iron between several phases and the complexity of diffraction patterns from iron carbides, reflections from iron-containing phases could not be detected. One can see, however, that no measurable changes occur in the MnO support under reaction conditions. This is in contrast to studies at higher conversion where extensive formation of spinel phases occurs (*19, 20*).

DISCUSSION: PHYSICAL CHARACTERIZATION

Owing to extensive support oxidation the ambient atmosphere during reduction of the HTC catalysts contains more water than during LTC catalyst reduction. The presence of water during reduction has been shown to promote mobility of oxides, and the transport of silica support to magnetite particle surfaces under wet reducing conditions has been demonstrated (*40*). Temperature-programmed reduction studies indicate that the iron-containing phases reduce before the support does (*41*). The result in the present case may be that manganese oxide is transported to the surface of reduced iron particles during the latter stages of reduction. The coverage would be lowest for the LTC catalyst, higher for the HTC catalyst, and highest for the fast-reduced HTC catalyst, based on the relative wetness of the ambient atmosphere during reduction. This agrees with the experimental observations. If enough MnO is transported there may result complete encapsulation of individual iron particles, and this would explain the retention of uncarbided iron in HTC catalysts. Corroborating evidence has also recently been reported by Jensen and Massoth (*11*). The partial covering of metal catalysts by titanium oxide is also well documented (*42*) and has been used to explain the so-called "strong metal–support interaction" (*43*). Surface promotion of supported Ru (*44*) and Rh (*45, 46, 47*) by MnO has also been proposed.

A conceptual model for the catalyst for-

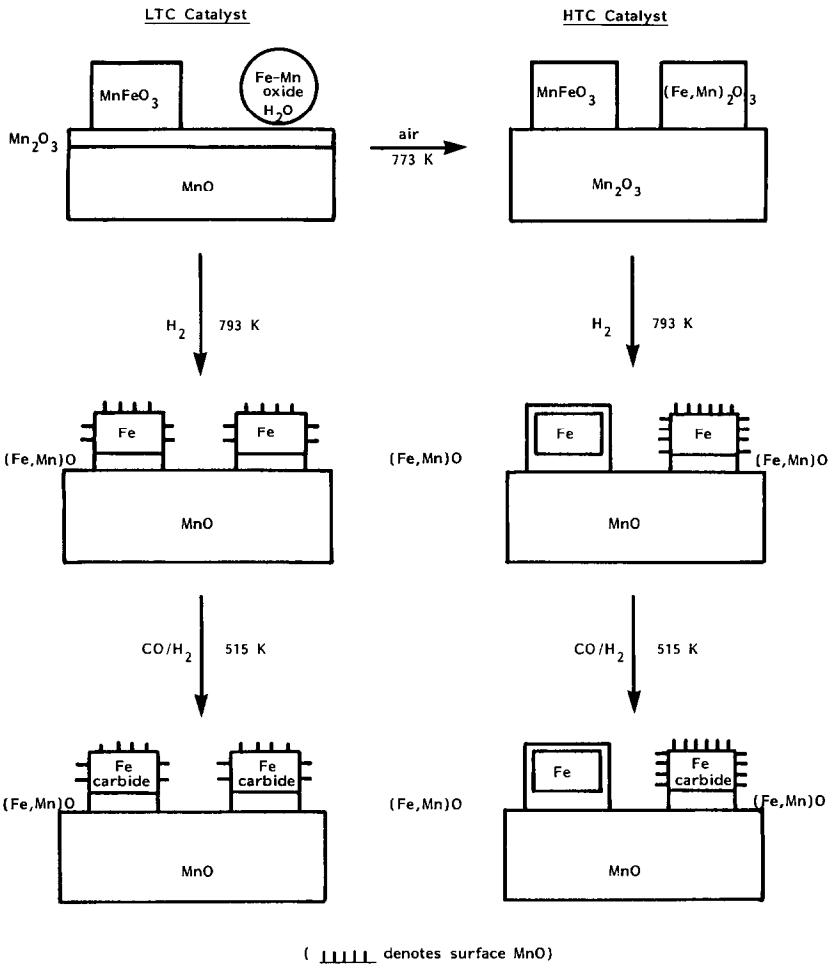

FIG. 15. A proposed model for Fe/MnO catalyst formation.

mation is proposed as illustrated in Fig. 15. The upper left represents the catalyst after impregnation, drying, and calcination at 474 K. This is the LTC catalyst. The support phase is predominantly MnO, with a surface layer of Mn_2O_3. Iron is present in particles of cubic $MnFeO_3$, and in hydrated FeMn oxide. Subsequent calcination at 777 K produces the HTC catalyst, dehydrating and crystallizing the hydrated mixed oxide to form hexagonal $(Fe,Mn)_2O_3$ and oxidizing the support to predominantly Mn_2O_3. For both the HTC and LTC materials, hydrogen pretreatment at 793 K results in nearly pure iron particles supported on MnO with (Fe,Mn)O at the interfaces. The iron surfaces are at least partially covered with MnO or (Fe,Mn)O, the degree of coverage being greater for HTC catalysts. Fast reduction, in particular, results in a large fraction of encapsulated iron particles. Exposure to synthesis conditions results in carburization of all nonencapsulated particles to a mixture of ε' and χ carbides, possibly converting a small fraction of the iron-metal to Fe(II) as (Fe,Mn)O.

CONCLUSIONS

The Fe/MnO catalysts of this study are catalytically different from unpromoted

iron catalysts, with high activity for water–gas shift, low selectivity for methane, low activity for the secondary hydrogenation of olefins, and low hydrogen uptake. It is concluded that MnO can promote low molecular weight olefin selectivity from the primary synthesis reaction, but at the expense of high CO_2 production. Similar conclusions are reported by Kim *et al.* (*36*) for Mn-promoted Raney iron.

A great deal of Fe–Mn interaction occurs in the calcined catalysts, but they segregate to a large extent during reduction. A significant amount of iron in the working catalyst is present as Fe(II), presumably in the phase identified as (Fe,Mn)O. Most of the rest remains unalloyed with manganese and forms carbide phases similar to those found in unpromoted iron catalysts.

Higher catalyst calcination temperature leads to lower activity, but stronger promotion. This is interpreted in terms of the amount of water present during reduction, which facilitates transport of MnO to the iron surface. In extreme cases encapsulation of some iron particles occurs.

Catalysts calcined at the higher temperature and reduced by the standard method exhibit atypical behavior at 515 K, which leads to unusually high C_2-C_4 hydrocarbon selectivity at higher pressure. This may be due to a strong interaction of the MnO-promoted surfaces with the reaction products CO_2 and H_2O. The effect is diminished at higher temperature, due to reduced strength of this interaction.

The lowered production of methane and higher olefin selectivity seem to be hallmarks of the FeMn system in various configurations, but at the expense of lower overall FT activity and high CO_2 production. It would be of great interest to test the HTC catalyst at higher CO conversions (but still at temperatures where its unusual selectivity may be exhibited) to see if the methane selectivity and the growth parameter above C_4 continue to decrease, and if there is formation of spinel phases.

The present catalysts unfortunately have a low support surface area, resulting in low iron dispersion even at 2% loading, small hydrogen uptake, low activity, and difficulties in relating the bulk physical characterization to the surface phenomena. Higher surface area MnO could probably be prepared by precipitation and reduction and one might reasonably expect even stronger interactions in such materials.

ACKNOWLEDGMENTS

We thank the Stauffer Chemical Company and the Mobil Foundation for general support of this work. Specific portions were assisted through NATO Grant 117/81, and KMK is particularly appreciative of discussions with Professor M. Baerns and associates at Ruhr-Universität Bochum in November–December 1984. JBB appreciates the support of the Alexander von Humboldt-Stiftung for completion of this work.

REFERENCES

1. Madon, R. J., *J. Catal.* **54,** 183 (1979).
2. Eigenbor, N. O., and Cooper, W. C., *Appl. Catal.* **14,** 323 (1985).
3. Huff, J. A., Jr., and Satterfield, C. N., *J. Catal.* **85,** 370 (1984).
4. Koenig, L., and Gaube, J., *Chem. Eng. Tech.* **55,** 14 (1983).
5. Koelbel, H., and Tillmetz, K. D., German Patent 2,507,647 (1976).
6. Koelbel, H., and Tillmetz, K. D., U.S. Patent 4,177,203 (1979).
7. Buessmeier, B., Frohning, C. D., and Cornils, B., *Hydro. Proc.* **11,** 105 (1976).
8. Buessmeier, B., Frohning, C. D., Horn, G., and Kluy, W., German Patents 2,518,964 and 2,536,488 (1976).
9. Barrault, J., Forquy, C., and Perrichon, V., *Appl. Catal.* **5,** 119 (1983).
10. Maiti, G. C., Malessa, R., Löchner, U., Papp, H., and Baerns, M., *Appl. Catal.* **16,** 215 (1985).
11. Jensen, K. B., and Massoth, F. E., *J. Catal.* **92,** 98 (1985).
12. Van Dijk, W. L., Niemantsverdriet, J. W., van der Kraan, A. M., and van der Baan, H. S., *Appl. Catal.* **2,** 283 (1982).
13. Deckwer, W. D., Lehmann, H. J., Ralek, M., and Schmidt, B., *Chem. Eng. Tech.* **53,** 819 (1981).
14. Deckwer, W. D., Serpemen, Y., Ralek, M., and Schmidt, B., *Ind. Eng. Chem. Proc. Des. Devel.* **21,** 222 (1982).
15. Satterfield, C. N., and Stenger, H. G., *Ind. Eng. Chem. Proc. Des. Devel.* **23,** 26, (1984).
16. Biloen, P., and Sachtler, W. M. H., "Advances in Catalysis," Vol. 30, p. 165. Academic Press, New York, 1981.

17. Arcuri, K. B., Schwartz, L. H., Piotrowski, R. D., and Butt, J. B., *J. Catal.* **85,** 349 (1984).
18. Kreitman, K. M., Ph.D. dissertation, Northwestern University, Evanston, IL 60201, June 1986. Available from University Microfilms, Inc.
19. Jaggi, N. J., Schwartz, L. H., Butt, J. B., Papp, H., and Baerns, M., *Appl. Catal.* **13,** 347 (1985).
20. Deppe, P., Papp, H., and Rosenberg, M., *Hyperfine Interact.* **28,** 903 (1986).
21. Dry, M. E., Shingles, T., and Boshoff, L. J., *J. Catal.* **25,** 99 (1972).
22. Anderson, R. B., *in* "Catalysis" (P. H. Emmett, Ed.), Vol. 4. Reinhold, New York, 1956.
23. Newsome, D. S., *Catal. Rev.* **21,** 275 (1980).
24. Amelse, J. A., Schwartz, L. H., and Butt, J. B., *J. Catal.* **91,** 241 (1985).
25. Yeh, E. G., Schwartz, L. H., and Butt, J. B., *J. Catal.* **91,** 241 (1985).
26. Leconte, M., Rojas, D., and Basset, J. M., *Nouv. J. Chim.* **8,** 69 (1984); see also Leconte, M., Theolier, A., and Basset, J. M., *J. Mol. Catal.* **28,** 217 (1985).
27. Arcuri, K. B., Ph.D. dissertation, Northwestern University, Evanston, IL 60201, June 1983. Available from University Microfilms, Inc.
28. Dwyer, D. J., and Somorjal, G., *J. Catal.* **56,** 2449 (1979).
29. Pichler, H., and Schulz, H., *Chem. Eng. Tech.* **42,** 1162 (1970).
30. Schulz, H., and Achtsnit, H. D., "Proc. 5th Iberoamer. Cong. Catal., 1976."
31. Malessa, R., and Baerns, M., *Ind. Eng. Chem. Proc. Des. Dev.,* in press.
32. Jacobs, P. A., and Van Wouwe, D., *J. Mol. Catal.* **17,** 145 (1982).
33. Anderson, J. K., "Structure of Metallic Catalysts." Academic Press, New York/London, 1975.
34. Le Caer, G., Dubois, J. M., and Senateur, J. P., *J. Solid State Chem.* **19,** 19 (1976).
35. Huffman, G. P., and Podgurski, H. H., *Acta Metall.* **23,** 1367 (1975).
36. Kim, C., Chen, K., Hanson, F. V., Oblad, A. G., and Tsai, Y., *Prepr. Amer. Chem. Soc., Div. Pet. Chem.* **31,** 198 (1986).
37. Raupp, G. B., and Delgass, W. N., *J. Catal.* **58,** 337 (1979).
38. Amelse, J. A., Schwartz, L. H., and Butt, J. B., *J. Phys. Chem.* **82,** 588 (1978).
39. Löchner, U., Papp, H., and Baerns, M., *Appl. Catal.* **23,** 339 (1986).
40. Lund, C. R. F., and Dumesic, J. A., *J. Catal.* **76,** 93 (1982).
41. Barrault, J., and Renard, C., *Appl. Catal.* **14,** 133 (1985).
42. Takatani, S., and Chung, Y-W., *Appl. Surf. Sci.* **19,** 341 (1984).
43. Tauster, S. J., Fung, S. C., and Garten, R. L., *J. Amer. Chem. Soc.* **100,** 170 (1978).
44. Kugler, E. L., Tauster, S. J., and Fung, S. C., U.S. Patent 4,206,134 (1980).
45. Ichikawa, M., Fukushima, T., and Shikakura, R., "Proceedings, 8th International Congress on Catalysis, Berlin, 1984. Dechema, Frankfurt-am-Main, 1984.
46. Van den Berg, Ph.D. dissertation, Leiden, June 1983.
47. Wilson, T. P., Kasai, P. H., and Ellegen, J., *J. Catal.* **69,** 193 (1981).